Scientific Journal of Astana IT University
ISSN (P): 2707-9031 ISSN (E): 2707-904X
VOLUME 25, MARCH 2026

DOI: **10.37943/25VGCQ1362**

Bolat Kassyiet
Student in Computer Science, Computing and Data Science
Department 232145@astanait.edu.kz, orcid.org/0009-0009-6907-8328
Astana IT University, Kazakhstan
Altynshash Rakhimzhanova
Master, Junior Researcher of Science and Innovation Center
"Big Data and Blockchain Technologies"
altynshash.rakhimzhanova@gmail.com, orcid.org/0009-0003-6052-8341
Astana IT University, Kazakhstan
Kudaibergen Zhanpeissov
Master student in Applied Data Analytics,
Computing and Data Science Department
242826@astanait.edu.kz, https://orcid.org/0009-0003-5178-794X
Astana IT University, Kazakhstan
Zheniskul Zhantassova
Candidate of Technical Sciences, Associate Professor,
Leading Researcher
zheniskul_z@mail.ru, orcid.org/0000-0001-5550-7587
Astana IT University, Kazakhstan
Anar Rakhimzhanova
Assistant Professor of Computing and Data Science, PhD
a.rakhymzhanova@astanait.edu.kz, orcid.org/0000-0003-4646-0603
Astana IT University, Kazakhstan

PHYSICALLY BASED EVALUATION OF SNOWPACK SENSITIVITY TO TEMPERATURE PERTURBATIONS IN EAST KAZAKHSTAN

Abstract: Seasonal snowpack is a critical regulator of water supply and flood risk in continental climates, yet its reliable assessment in Central Asia is constrained by sparse observations. This study applies the multilayer Snow Thermal Model, driven by ERA5-Land reanalysis, to simulate snowpack evolution in East Kazakhstan during the 2022-2023 season and evaluates its performance against snow depth and snow water equivalent observations from the Kazhydromet network.

The model reproduced snow accumulation, peak storage, and melt onset with high accuracy, achieving explained variance above 90%. Importantly, analysis of energy fluxes and stratigraphy revealed that more than half of simulated meltwater was produced under subfreezing air temperatures. Snowmelt is primarily controlled by positive surface energy balance dominated by net radiation and turbulent heat fluxes.

Perturbation experiments further highlight the disproportionate sensitivity of the snow regime to modest thermal changes. A uniform +2 °C warming reduced peak snow water equivalent by nearly one third and advanced melt onset by two to three weeks, while a −1 °C cooling increased snow storage and prolonged snow duration. These threshold-driven responses show that even small climatic deviations or biases in forcing data can shift runoff timing and seasonal water availability. For water managers, this implies that operational planning must explicitly account for temperature sensitivity, since minor departures from average conditions can trigger substantial changes in spring flood risk.

Overall, the study demonstrates that reanalysis-driven, physically based snow modeling provides robust diagnostics in data-scarce regions, surpassing empirical methods in both accuracy and explanatory power. The findings establish its importance for climate sensitivity analysis, flood preparedness, and water resource planning in snow-dominated basins.

Keywords: Climate change; Hydrological forecasting; Physically based models; Snow Thermal Model.

Received: 03.09.2025 Accepted: 25.02.2026 Published: 30.03.2026

DOI: 10.37943/25VGCQ1362

Introduction

In snow-dominated basins, the seasonal snowpack acts as a natural reservoir-storing winter precipitation and releasing it as meltwater during spring. The timing and intensity of this melt govern water supply, reservoir operation, and flood hazards [1-3]. In continental cold regions such as Central Asia, snowmelt is particularly abrupt due to steep winter-to-spring temperature gradients, creating a high risk of flash floods, infrastructure damage, and ecological disruption [4]. Reliable snowpack modeling is therefore indispensable for both hydrological forecasting and climate adaptation planning.

Despite decades of model development, snow simulation in data-scarce regions remains challenging. Empirical approaches such as the Degree-Day Factor (DDF) method are widely used due to their simplicity, but they rely solely on air temperature thresholds and cannot represent internal snowpack processes. In contrast, physically based models such as SNTHERM, CROCUS, and SnowModel simulate coupled heat and mass transfer through multilayer snow profiles, accounting for conduction, compaction, phase change, grain metamorphism, and meltwater percolation [5]. However, their adoption in Central Asia has been limited by sparse observations and a lack of reliable meteorological forcing [6-7].

Ground-based observations provided by Kazhydromet, the national hydrometeorological service of Kazakhstan, remain the primary reference for snow depth and meteorological conditions in the region. These measurements are valuable but constrained by their 10-day (decadal) observation frequency, which may limit temporal resolution and lead to mismatches when compared against continuous model or reanalysis outputs. Nevertheless, they serve as an essential benchmark for model validation, offering independent verification of simulated snowpack dynamics.

Recent advances in reanalysis products, particularly ERA5-Land, provide high-resolution and physically consistent meteorological forcing data that can help overcome these barriers [8]. ERA5-Land has already demonstrated value for hydrological and cryospheric studies in under-monitored regions [9–10], yet its potential for driving physically based snow models in Central Asia remains largely unexplored.

In the work of Daly S.F., Giovando J., Hamill D., Dahl T., and Bartles M., the authors applied an empirical approach to simulate snowmelt dynamics in mountainous basins [11]. This approach is based mainly on air temperature thresholds and has been widely used due to its simplicity and low input requirements. However, as highlighted by Zhou G., Chen W., and Chen K., such empirical formulations neglect radiative fluxes, snow layering, and percolation processes, which often leads to reduced accuracy in regions with high interannual climate variability [12].

Lafaysse M. et al. presented a physically based snow modelling framework that represents multilayer snowpack dynamics, including heat transfer, compaction, liquid water percolation, and snow microstructure evolution [13]. Similarly, Le Moigne P., Besson F., Martin E. et al. described improvements in a hydrometeorological modelling system for France, demonstrating its usefulness for representing snow-related land-surface and energy-exchange processes [14]. Kim R.S., Kumar S., Vuyovich C. et al. applied ensemble land-surface modelling across North America to quantify snow water equivalent uncertainty under large-scale atmospheric forcing [15].

Hao X., Huang G., Zheng Z. et al. developed a new MODIS-based snow-cover-extent product over China by combining Terra and Aqua MODIS observations with cloud-gap-filling procedures [16]. Validation against ground meteorological stations demonstrated high snow-mapping accuracy, while the remaining uncertainties were mainly associated with cloud cover and topographic complexity. Wrzesien M.L., Durand M.T., Pavelsky T.M. et al. presented a continental-scale assessment of mountain snow accumulation over North America, emphasizing the value of model-based estimates in regions with sparse observations [17]. Bonsoms J., López-Moreno J.I., Lemus-Canovas M., and Oliva M. examined future winter snowfall and extreme snow events in the Pyrenees, highlighting how spatial heterogeneity and climate sensitivity complicate snow assessment and model transferability [18].

The aim of the analysis is to demonstrate that the physically based Snow Thermal Model, when coupled with ERA5-Land reanalysis, can reliably reproduce snowpack dynamics in East Kazakhstan and provide mechanistic insight into melt processes beyond what empirical models can capture. Specifically, the results are intended to (i) validate the model's ability to reproduce observed snow depth and snow water equivalent, (ii) identify the dominant physical drivers of meltwater generation, including processes occurring under subfreezing air temperatures, and (iii) quantify the snowpack's sensitivity to modest thermal

Scientific Journal of Astana IT University
ISSN (P): 2707-9031 ISSN (E): 2707-904X
VOLUME 25, MARCH 2026

perturbations. Through these steps, the study evaluates not only the accuracy of the model but also its practical relevance for hydrological forecasting, flood preparedness, and climate impact assessment in data-scarce continental regions.

Methods and Materials

1. Study Area and Forcing Data

This study focuses on the seasonal evolution of the snowpack in East Kazakhstan, a region with a sharply continental climate characterized by cold winters, low winter precipitation, and rapid warming in spring. The selected site lies within the Irtysh River basin, one of the most important transboundary river systems in Central Asia, which plays a critical role in regional water supply, hydropower generation, and ecosystem functioning. Snowmelt runoff from this basin contributes substantially to spring flood generation and downstream water availability.

The district of Shymonaikha, located within the Irtysh catchment, was chosen as the study site. The area is typically snow-covered from early November until late March, with maximum snow depths reaching 30-40 cm during the 2022-2023 winter season. Average January air temperatures are around -15 °C, with frequent cold spells below -25 °C. Total winter precipitation is generally modest (60-90 mm), falling mainly as snow. Fig. 1 shows a lake in Uba during winter. The frozen surface and extensive surrounding snow cover illustrate the dominance of winter conditions and highlight the importance of snowpack as a seasonal water reservoir in this region.

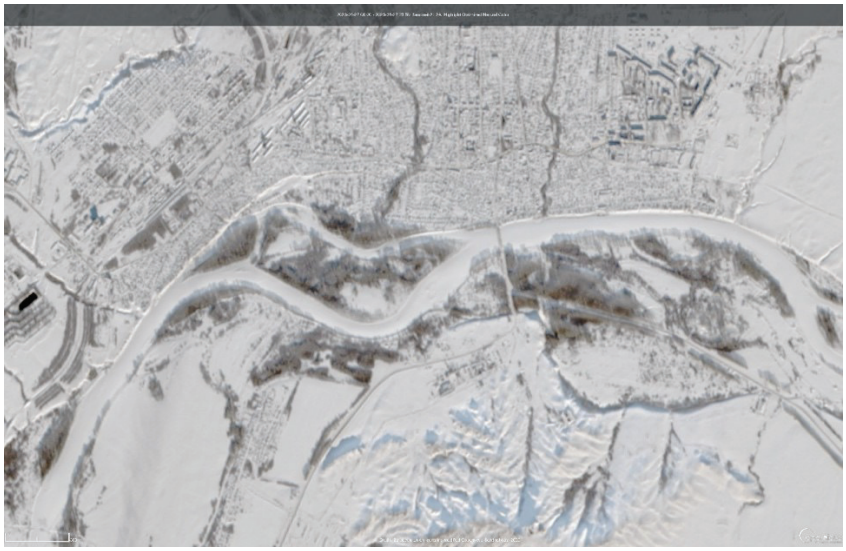

Figure 1. Satellite image of the Uba River

The basin is dominated by snowmelt-driven hydrology, with seasonal snowpack acting as the primary water storage. Snow accumulation typically begins in late October, peaks in February–March, and melts rapidly in April, generating high spring runoff. This dynamic makes the region especially vulnerable to snowmelt-induced flooding, which poses risks to settlements and infrastructure along the Irtysh.

All simulations were driven exclusively by ERA5-Land reanalysis, which provides hourly meteorological fields at approximately 0.1° spatial resolution. Meteorological forcing for SNTHERM simulations was derived directly from ERA5-Land without bias correction. Local station observations from Kazhydromet were used only for independent comparison and validation and were not used to adjust or bias-correct model forcing fields. This ensures independence between forcing data and validation observations. ERA5-Land was selected because it offers consistent temporal coverage and physically coherent surface variables, which is critical in regions where ground observations are sparse or limited to decadal snow surveys. Data were extracted for the grid cell coinciding with the study site and resampled, where necessary, to match the model timestep. The input variables supplied to SNTHERM are summarized in Table 1. These represent the minimum physical set required to resolve snowpack energy and mass exchange.

DOI: 10.37943/25VGCQ1362

Table 1. Meteorological input variables used to force the SNTHERM model

Variable	Units	Description
2 m air temperature	K	Main driver of melt and phase partitioning
2 m relative humidity	%	Influences vapor flux and latent heat
10 m wind speed	$m\ s^{-1}$	Affects turbulent heat exchange
Incoming shortwave radiation	$W\ m^{-2}$	Solar energy input to snow surface
Incoming longwave radiation	$W\ m^{-2}$	Atmospheric longwave forcing
Total precipitation	$m\ h^{-1}$	Partitioned into rain/snow based on T
Surface pressure	Pa	Required for thermodynamic calculations

Precipitation was divided into snowfall and rainfall using a fixed 0 °C air temperature threshold, following standard practice in snow-hydrology studies. All variables were ingested at hourly resolution, ensuring physically consistent forcing of mass and energy exchange at the snow-atmosphere interface.

SNTHERM was initialized on 1 October 2022 with bare-ground conditions. Soil parameters were specified as sandy loam, representative of the regional substrate. The model then simulated the full winter season, resolving snow stratigraphy and energy balance processes including heat conduction, densification, liquid water retention and percolation, refreezing, and grain metamorphism. This physically explicit setup ensures that the simulations reflect both the timing and intensity of snow accumulation and melt in a process-consistent manner, rather than relying on empirical melt factors.

To evaluate model skill, simulated snow depth (SD) from the baseline experiment was compared against in situ observations provided by Kazhydromet, the national hydrometeorological service of Kazakhstan. These observations are based on routine manual snow surveys conducted at the reference station. The original records are available at decadal intervals and were used as the native temporal resolution for validation analysis. Model performance metrics were calculated using model outputs sampled directly at observation timestamps, without temporal interpolation. Despite their coarse temporal sampling, these measurements represent the only independent ground reference in the region and therefore provide a critical benchmark for model validation and subsequent sensitivity experiments with perturbed temperature forcing.

2. SNTHERM Model Setup

The SNTHERM (Snow Thermal Model**)** is a one-dimensional, multi-layer, physically based numerical model developed by the U.S. Army Cold Regions Research and Engineering Laboratory (USACRREL) to simulate the thermal evolution of snow and soil under atmospheric forcing. The model has been widely applied in both research and operational contexts owing to its ability to resolve key processes such as heat conduction, melt-refreeze cycles, and liquid water percolation with high temporal and vertical resolution. Its formulation explicitly incorporates the dominant thermodynamic and hydrological mechanisms that control snowpack accumulation, metamorphism, and ablation. These processes are summarized in Table 2.

Table 2. Physical processes represented in the SNTHERM model

Process	Description
Thermal conduction	Heat transfer within and between snow, ice, and soil layers
Phase changes	Melting, refreezing, and sublimation, with latent heat exchange
Snow compaction	Densification due to overburden pressure and temperature-driven metamorphism
Liquid water transport	Percolation of meltwater, capillary retention, and drainage
Grain-type transitions	Evolution of snow microstructure affecting thermal and mechanical properties

For diagnostic purposes, the following output variables were extracted from SNTHERM (Table 3). These variables provide key indicators of snowpack state and melt dynamics and serve as the basis for model validation and sensitivity analysis.

Scientific Journal of Astana IT University
ISSN (P): 2707-9031 ISSN (E): 2707-904X
VOLUME 25, MARCH 2026

Table 3. Key model outputs extracted from SNTHERM simulations

Output Variable	Units	Description
Snow Water Equivalent	mm	Total water-equivalent snow mass above ground
Snow depth	m	Geometric thickness of the snowpack
Snow temperature profiles	K	Vertical temperature distribution through the snow layers
Liquid water content	%	Fraction of meltwater held in the snowpack
Surface energy fluxes	W m^{-2}	Includes net radiation, sensible, latent, and ground heat fluxes

SNTHERM discretizes the snow-soil column into a series of layers, each defined by state variables including temperature (T), density (ρ), porosity (ϕ), liquid water content (θw), and grain structure (G). The temporal evolution of these variables is governed by the coupled conservation of energy and mass. The model dynamically regrids the column to resolve fine-scale processes such as melt-refreeze cycles and rain-on-snow events [19].

The governing equations of SNTHERM follow directly from conservation principles. At the snow-atmosphere interface, the upper boundary is defined by the net surface energy balance [20].

$$Q_{net} = (1-\alpha)Q_s + Q_{lw}^{\downarrow} - Q_{lw}^{\uparrow} + Q_h + Q_e + Q_g , \quad (1)$$

where Q_{net} - net energy flux at the snow surface , Q_s - incoming shortwave radiation, α - snow albedo, $Q_{lw}^{\downarrow}$, $Q_{lw}^{\uparrow}$ - downwelling and upwelling longwave radiation, Q_h - sensible heat flux, Q_e- latent heat flux, Q_g- ground heat flux at the snow-soil interface .

Within the snowpack, heat conduction is coupled with latent heat release and absorption due to phase change

$$C_i \frac{\partial T_i}{\partial t} = \frac{\partial}{\partial z}(k_i \frac{\partial T_i}{\partial z}) + L_f \frac{\partial \theta_w}{\partial t} , \quad (2)$$

where C_i - volumetric heat capacity of layer i, k_i- thermal conductivity of layer i, T_i - temperature, z - vertical depth, L_f - latent heat of fusion, θ_w - liquid water content. This formulation explicitly couples sensible heating with phase-change latent heat release/absorption.

Snow densification is expressed through a temperature- and stress-dependent creep law that captures both mechanical settlement and thermally activated compaction

$$\frac{\partial p}{\partial t} = C_1 \rho g \exp(k_i \frac{E}{\partial z}) + L_f \frac{\partial \theta_w}{\partial t} , \quad (3)$$

where ρ - snow density, g - gravitational acceleration, R - universal gas constant, E_a- activation energy for creep, C_1, C_2 - empirical parameters for mechanical and thermal compaction, T_0 - reference temperature.

The vertical redistribution of meltwater is described using Darcy's law for unsaturated flow

$$q = -K(\theta)(\frac{\partial \psi}{\partial z} + 1) . \quad (4)$$

Here q - water flux, K(θ) - hydraulic conductivity, Ψ - matric potential. This formulation captures retention in pore spaces, percolation through stratigraphy, and ultimate drainage from the pack.

Together, these formulations provide a physically consistent framework for snowpack evolution, capturing surface radiative and turbulent exchanges, conductive-latent heat coupling, densification under stress and temperature forcing, and the redistribution of liquid water. This process-based representation contrasts with empirical degree-day approaches, offering greater transferability to data-scarce regions and improved robustness under non-stationary climate conditions.

DOI: 10.37943/25VGCQ1362

3. Model Implementation and Validation

For this study, SNTHERM was initialized on 1 October 2022 with bare-ground, snow-free conditions. Meteorological forcing was obtained from ERA5-Land at hourly resolution and included air temperature, precipitation, humidity, wind speed, and radiative fluxes. Precipitation was partitioned into snowfall and rainfall using a 0 °C threshold [21]. The lower boundary condition was set as a constant soil temperature at depth, allowing conductive heat exchange. The soil was parameterized as sandy loam, following standard mid-latitude loam profiles [22], while snow thermal and optical properties were taken from the default SNTHERM configuration. Snowpack stratigraphy evolved dynamically, with adaptive regridding to capture sharp vertical gradients in temperature, density, and liquid water.

The diagnostic outputs, SWE, snow depth, liquid water content, vertical temperature profiles, and surface fluxes. were analyzed for the full October-April simulation period to capture both accumulation and ablation phases.

For validation, simulated SWE was compared against observational data obtained from Kazhydromet's manual snow surveys at the meteorological station. Observations, originally measured at weekly intervals, were linearly interpolated to daily resolution for consistency with model outputs. Validation was performed using standard statistical metrics, including

$$Bias = \frac{1}{N}\sum_{i=1}^{N}(SWE_i^{\mathrm{mod}} - SWE_i^{obs}), \tag{5}$$

$$RMSE = \sqrt{\frac{1}{N}\sum_{i=1}^{N}(SWE_i^{\mathrm{mod}} - SWE_i^{obs})^2}, \tag{6}$$

$$R^2 = 1 - \frac{\sum_{i=1}^{N}(SWE_i^{\mathrm{mod}} - SWE_i^{obs})^2}{\sum_{i=1}^{N}(SWE_i^{obs} - SWE_i^{obs})^2}, \tag{7}$$

where SWE^{mod} and SWE^{obs} denote modeled and observed snow water equivalent, respectively. These indices quantify both absolute error and explained variance, allowing for a rigorous evaluation of model performance [23].

4. Degree-Day Factor (DDF) Method for Melt Estimation

The Degree-Day Factor (DDF) method remains one of the most widely applied approaches for snowmelt estimation in operational hydrology, particularly in regions with limited meteorological data [24]. The method assumes a linear relationship between air temperature above a threshold and daily melt rates, thereby bypassing the need for energy balance calculations. Despite its simplicity, the DDF method has demonstrated practical reliability in large-scale hydrological models and flood forecasting systems [25-26]. Daily melt was estimated using the standard formulation

$$M(t) = DDF * \max(T_\alpha(t) - T_{base}, 0), \tag{8}$$

where M(t) is melt (mm day^{-1}), T_a(t) is mean daily air temperature (°C), T_{base} is the melt threshold (set to 0 °C), and DDF (mm °C^{-1} day^{-1}) is an empirical coefficient calibrated for site conditions.

In this study, SNTHERM-derived melt (calculated as daily SWE decreases during the ablation season, where sublimation losses are expected to be small relative to melt during peak ablation periods) was used to calibrate a site-specific DDF by minimizing RMSE between cumulative SNTHERM melt and cumulative empirical estimates. The calibrated DDF was then applied to ERA5-Land air temperature to generate an independent empirical melt series. Comparisons focused on melt onset, peak melt rates, cumulative melt volumes, and ablation duration. This procedure highlights both the practicality of DDF in data-scarce regions and the added diagnostic value of SNTHERM in resolving internal snowpack processes.

Scientific Journal of Astana IT University
ISSN (P): 2707-9031 ISSN (E): 2707-904X
VOLUME 25, MARCH 2026

5. Temperature Sensitivity Simulations

Air temperature is the primary external control on seasonal snowpack evolution in continental cold regions. It governs precipitation phase partitioning, regulates melt onset through its influence on the surface energy balance, and affects snow densification and liquid water retention processes. In climates where winter and spring temperatures frequently fluctuate near the freezing point, small temperature deviations can produce disproportionate changes in snow accumulation, melt timing, and seasonal water storage. To quantify snowpack sensitivity to realistic thermal perturbations, a set of additive temperature-offset experiments was performed using the SNTHERM model. Instead of multiplicative percentage scaling, perturbations were applied as fixed temperature offsets to ensure physical interpretability and comparability with established climate-sensitivity studies.

Four scenarios were simulated using identical meteorological forcing except for near-surface air temperature:

- Baseline (0 °C offset): Original ERA5-Land temperature forcing
- Cooling (−1 °C): Uniform decrease in air temperature
- Mild warming (+1 °C): Uniform increase in air temperature
- Stronger warming (+2 °C): Uniform increase in air temperature.

Temperature perturbations were applied as additive offsets to near-surface air temperature only (equivalent to −1 to +2 K in model forcing units). All other meteorological variables, including precipitation, incoming shortwave radiation, incoming longwave radiation, wind speed, relative humidity, and surface pressure, were kept unchanged. This experimental design was selected for three main reasons. First, additive temperature offsets are widely used in cryospheric and hydrological climate sensitivity studies because absolute temperature differences directly control precipitation phase partitioning and snowpack energy exchange processes. Second, this formulation provides direct comparability with projected regional warming magnitudes, which are typically expressed in degrees Celsius rather than relative percentage changes. Third, additive perturbations avoid ambiguity when forcing data are expressed in Kelvin, where percentage scaling can produce unrealistically large absolute temperature changes. Applying perturbations to air temperature only allows isolation of the direct thermodynamic influence of temperature on snowpack evolution. Although longwave radiation is physically coupled to atmospheric temperature through radiative transfer processes, it was intentionally kept unchanged in this study. This approach avoids introducing secondary radiative feedbacks and is consistent with first-order temperature sensitivity experiment design commonly used in physically based snow modeling.

This methodology is particularly relevant for continental regions such as East Kazakhstan, where winter temperatures frequently oscillate near the freezing threshold. Under such conditions, small temperature shifts can significantly alter snowfall retention, snow metamorphism, and melt onset timing, resulting in nonlinear snowpack responses. Simulations were conducted for the period 1 October 2022 – 30 April 2023 using hourly ERA5-Land forcing data, with model outputs aggregated to daily resolution for analysis. Key snowpack indicators, including peak snow water equivalent (SWE), accumulation onset, melt initiation, and complete snow disappearance timing, were extracted for each scenario and compared relative to the baseline simulation. This experimental framework provides a controlled basis for quantifying threshold-driven snowpack sensitivity to realistic climate warming magnitudes in continental snow-dominated basins.

Results

The evaluation of SNTHERM simulations against in situ observations demonstrates that the physically based model provides a robust representation of snowpack dynamics in the continental climate of East Kazakhstan. Fig. 2 compares simulated and observed daily snow depth together with near-surface air temperature for November 2022-April 2023. Observed air temperature was obtained from the KazHydromet station and reported at approximately 10-day (decadal) intervals. Station observations were used only for independent comparison and validation and were not used to adjust model forcing fields. SNTHERM-simulated snow depth (black line, shaded) aligns closely with observed records (red dots), capturing both the seasonal cycle and the magnitude of accumulation. The model successfully reproduces the onset of snow cover in early winter, maintains realistic peak depths in mid-winter, and simulates the rapid spring melt-out with only minor phase deviations.

DOI: 10.37943/25VGCQ1362

Model validation was additionally performed against observed SWE time series. Snow depth observations are presented to illustrate seasonal structural evolution, while quantitative validation metrics are primarily reported for SWE. Validation metrics were calculated using model outputs sampled at observation timestamps.

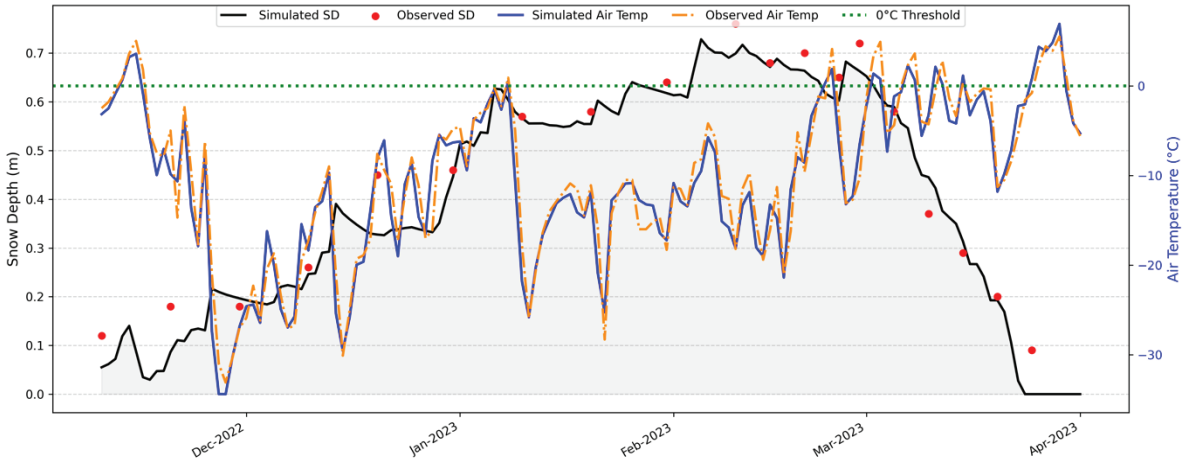

Figure 2. SNTHERM-simulated (black line, grey shading) vs. observed (red dots) daily snow depth and simulated (grey line) vs. observed (orange dashed) air temperature

Similarly, the comparison of simulated (blue solid) and observed (orange dashed) air temperatures shows that the model skillfully represents synoptic-scale variability and extreme events. The close correspondence between forcing data and station measurements highlights the suitability of ERA5-derived meteorological inputs for driving physically based snow models in data-sparse regions. Model validation was performed using in situ snow depth observations from Kazhydromet and SWE observations where available. Validation metrics were calculated using model outputs sampled at observation timestamps only. For the period November 2022 to April 2023 (n = 18), simulated snow depth showed strong agreement with observations (RMSE = 0.10 m, bias = +0.05 m, NSE = 0.78, R^2 = 0.85.

Early winter (November-December 2022): Snow accumulation begins in late November, coinciding with sustained air temperatures below the 0 °C threshold (green dotted line). Both simulated and observed snow depth show modest buildup (~0.1-0.2 m). The model slightly underestimates isolated observed snow events, which may reflect subgrid variability or precipitation undercatch at local stations. Nevertheless, the general agreement in timing and magnitude indicates that SNTHERM accurately initiates snowpack formation once temperature consistently drops below freezing.

Mid-winter (January-February 2023): During January, the snow depth steadily increases and stabilizes in February at approximately 0.6–0.7 m, while air temperatures remain consistently below the 0 °C threshold. The model captures the stable snow cover plateau, reflecting both reduced melt and effective accumulation processes. Short-term temperature oscillations are evident, yet they do not cross the green line, indicating limited melt activity. Both simulated and observed air temperatures exhibit very similar daily variability, reinforcing the ability of ERA5-driven forcing to represent regional temperature dynamics when compared with independent local station observations.

Late winter to early spring transition (March 2023): In March, air temperatures frequently oscillate around the 0 °C threshold. This transitional period is marked by repeated thaw-freeze cycles that strongly influence snowpack dynamics. The observed snow depth indicates gradual decreases beginning mid-March, while the model simulates a more continuous depletion starting slightly earlier. Despite minor timing discrepancies, the model realistically represents the onset of melt in response to threshold crossings.

Spring melt-out (late March-April 2023): A rapid decline in snow depth occurs as air temperatures remain persistently above 0 °C. The model shows complete melt-out by early April, consistent with observed disappearance of snow cover. The synchronization of simulated temperature with the green line highlights SNTHERM's sensitivity to thermal conditions driving ablation processes.

Scientific Journal of Astana IT University
ISSN (P): 2707-9031 ISSN (E): 2707-904X
VOLUME 25, MARCH 2026

Overall, the 0 °C threshold provides a clear diagnostic of snowpack response: below-freezing conditions support steady accumulation and stabilization (November-February), while repeated crossings around March initiate melt cycles, culminating in rapid ablation once temperatures remain positive. This threshold-driven response demonstrates the physical realism of SNTHERM, which contrasts with the linearity of degree-day factor (DDF) methods. The high agreement with observed dynamics highlights the model's transferability to data-scarce continental basins, where physically based approaches can significantly improve snow hydrology assessments compared to empirical methods.

In addition to reproducing observed snow depth dynamics and air temperature variability (Fig. 2), SNTHERM provides valuable insights into the physical drivers of snowmelt processes. Fig. 3 presents the distribution of cumulative simulated snowmelt by air temperature bins for the late winter-spring period (≥15 February 2023). A key outcome is that the majority of meltwater production occurs at subzero air temperatures (<0 °C), with the largest contributions in the < -5 °C and -5 to 0 °C ranges. This pattern indicates that melt is not solely a function of positive air temperature, as assumed in degree-day models, but is instead strongly dominated by radiative and turbulent energy fluxes, with snow metamorphism modifying snowpack properties that regulate melt efficiency. Under clear-sky conditions, absorbed shortwave radiation can induce melt even when ambient air remains below freezing, while longwave radiation and ground heat fluxes also contribute to energy inputs within the snowpack. SNTHERM captures these processes explicitly through its energy-balance framework, which explains the substantial subzero melt contributions observed in the simulation.

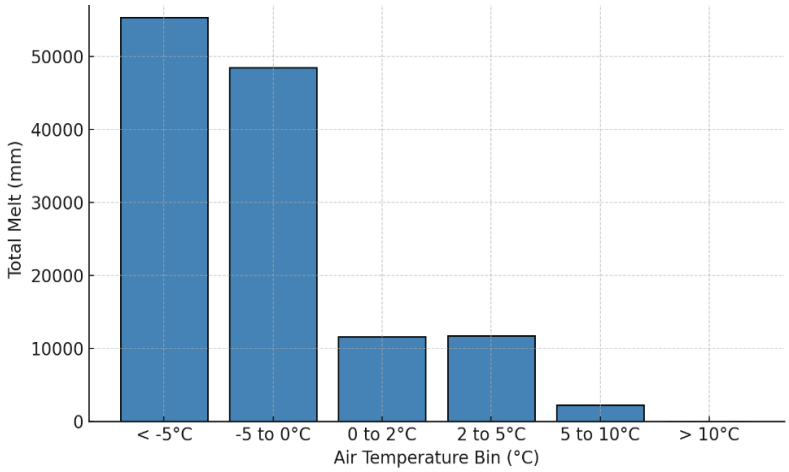

Figure 3. Cumulative snowmelt by air temperature bin (≥15 Feb 2023), with dominant subzero contributions.

At near-zero and slightly positive air temperatures (0 to 5 °C), melt contributions remain significant but secondary compared to the subzero regime. Beyond 5 °C, the contribution sharply decreases, reflecting the relatively short duration of sustained warm periods in this continental climate during late winter and early spring. This distribution highlights the limitations of temperature-index (degree-day factor) methods, which would misrepresent the timing and magnitude of snowmelt by neglecting radiation-driven processes under subfreezing conditions.

The temperature-binned melt analysis highlights an important insight into SNTHERM's process-based melt representation. Notably, the majority of cumulative meltwater generation occurred at subzero air temperatures, with approximately 55-60% of total melt produced below 0°C, and the largest single contribution from the <-5°C bin (Fig. 3).

Building on the snow depth and melt dynamics illustrated in Fig. 2 and Fig. 3, the internal evolution of the snowpack is further examined through liquid water content. This variable provides direct evidence of when the snowpack transitions from a dry, frozen state to an isothermal, melt-producing system.

Fig. 4 presents the SNTHERM-simulated evolution of liquid water fraction (%) within the snowpack during late winter 2023. For most of February, the snowpack remains dry, with liquid water fractions near zero. On 25 February 2023, the model detects the first significant appearance of liquid water (about 4%),

DOI: 10.37943/25VGCQ1362

marking the melt onset date. This is the transition point at which the snowpack begins to release meltwater, even though average air temperatures remain close to or below 0 °C.

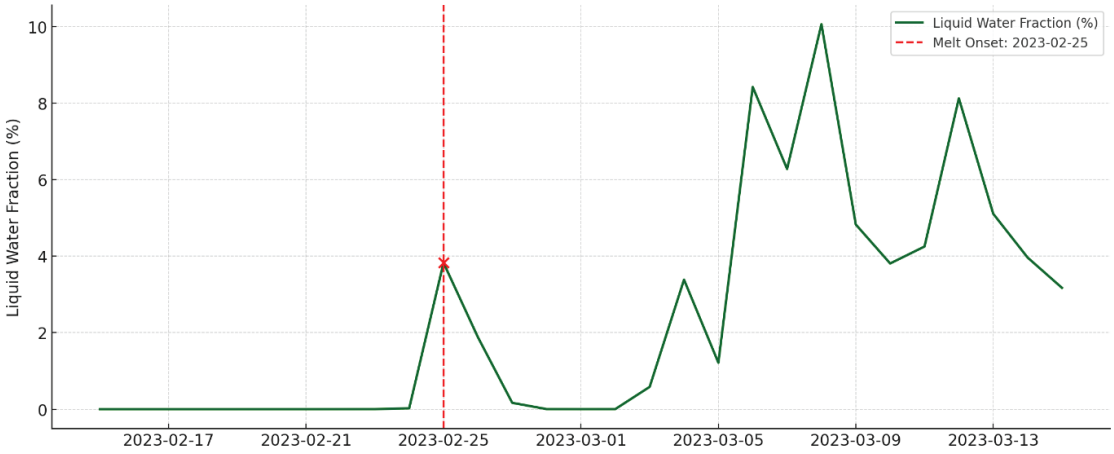

Figure 4. SNTHERM-simulated liquid water fraction (%) with melt onset on 25 February 2023.

After this onset, liquid water fractions fluctuate in early March, reflecting alternating thaw-freeze cycles where meltwater production is followed by refreezing during colder nights. From the first week of March onward, the liquid water fraction rises more consistently, exceeding 8-10% by mid-March. This indicates the development of a ripening snowpack, where pore spaces within the snow become saturated, enabling sustained meltwater percolation.

By mid-March, the snowpack has entered a state of continuous melt, consistent with the decline in snow depth observed in Fig. 5. The increasing liquid water content highlights the transition from a cold, dry snowpack to an isothermal snowpack, where internal energy balance processes dominate and accelerate ablation.

While liquid water fraction highlights the onset and internal progression of melt within the snowpack, the degree-day approach provides an external, temperature-based perspective on melt intensity. To complement the process-based SNTHERM outputs, cumulative Degree-Day Factor (DDF) melt is used to identify the timing and magnitude of major melt events across the season.

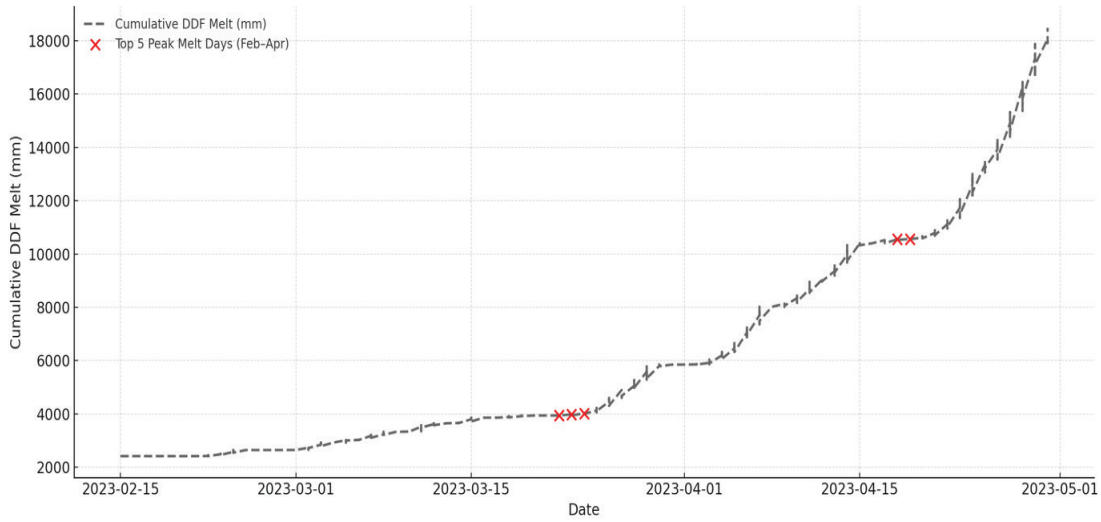

Figure 5. Cumulative DDF melt with top five peak days.

The degree-day framework thus complements physically based modeling by providing a simple but robust means to identify critical melt days with heightened hydrological significance.

Scientific Journal of Astana IT University
ISSN (P): 2707-9031 ISSN (E): 2707-904X
VOLUME 25, MARCH 2026

To assess the sensitivity of SNTHERM to thermal forcing, simulations were conducted under three scenarios: the baseline (0 °C), a warming perturbation (+2 °C), and a cooling perturbation (-1°C). All other meteorological inputs were held constant. Snow Water Equivalent (SWE) was derived from model outputs using the standard formulation:

$$SWE = \sum_{i=1}^{n} \rho_w^{-1} * \rho_{b,i} * \square \quad , \tag{9}$$

where ρ_w^{-1} is the bulk density of the i^{th} snow layer, Δz_i is its thickness, and ρ_w is the density of water. This formulation converts the vertical snow stratigraphy into equivalent water depth, enabling quantitative comparison with ground-based observations.

The baseline (0%) simulation showed a high degree of agreement with the observed seasonal SWE evolution, as confirmed by regression analysis. As shown in Fig. 6, simulated SWE correlates strongly with observations (R^2 = 0.917), indicating SNTHERM's robust capability in capturing snow accumulation and ablation dynamics under continental climatic conditions. The best-fit regression line lies close to the 1:1 line, suggesting minimal systematic bias across the range of SWE magnitudes. Some divergence was noted at higher SWE values, where simulations tend to slightly underestimate peak conditions. This discrepancy can be partly attributed to mismatches in temporal resolution: Kazhydromet provides decadal snow observations, while ERA5-Land inputs offer daily temporal granularity, which may smooth over transient peaks in the observed data. Nonetheless, the model effectively reproduces the phenological timing of accumulation onset, peak SWE, and snowmelt initiation.

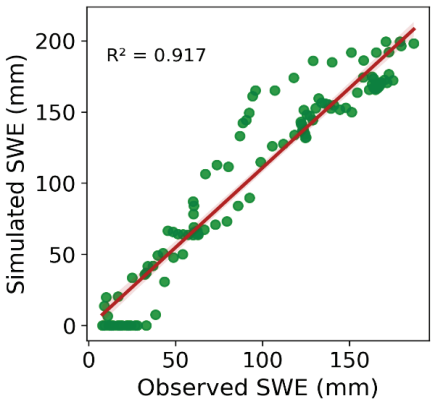

Figure 6. Regression of simulated SWE (SNTHERM, 0°C scenario) against observed SWE (Kazhydromet).

The temperature perturbation experiments demonstrate a strong and nonlinear sensitivity of snow water equivalent (SWE) to small thermal shifts (Fig. 7). The baseline simulation (0 °C offset) produced a peak SWE of approximately 236 mm in early March. Cooling by -1 °C increased peak SWE to approximately 245 mm, reflecting enhanced snowfall retention and reduced mid-winter melt losses. In contrast, warming scenarios produced substantial reductions in snow storage. The +1 °C scenario reduced peak SWE to approximately 219 mm, while the +2 °C scenario resulted in a pronounced decline to approximately 141 mm. These results indicate that warming produces disproportionately larger reductions in snow storage compared to the gains produced by equivalent cooling. Relative to the baseline simulation, the +2 °C warming scenario reduced peak SWE by approximately 35-40%, whereas the -1 °C cooling scenario increased peak SWE by only about 3-5%.

Temperature perturbations also significantly influenced seasonal snowpack timing. During the early accumulation period (November-December), the -1 °C scenario produced more rapid SWE buildup due to enhanced snowfall retention and reduced melt losses. Conversely, the +2 °C scenario delayed effective snow accumulation and reduced early-season SWE storage. During late winter and early spring, warming scenarios accelerated melt onset and snowpack depletion, while cooling delayed the transition to sustained melt conditions and prolonged snow cover duration.

DOI: 10.37943/25VGCQ1362

The asymmetric response between warming and cooling scenarios highlights the threshold-controlled nature of snowpack evolution. Near-freezing temperature conditions strongly influence precipitation phase partitioning and surface energy balance processes. Small temperature increases promote rainfall instead of snowfall and enhance melt energy availability, resulting in rapid snowpack depletion. These results confirm that snowpack evolution in continental climates cannot be approximated as a linear function of temperature, particularly during late winter transition periods.

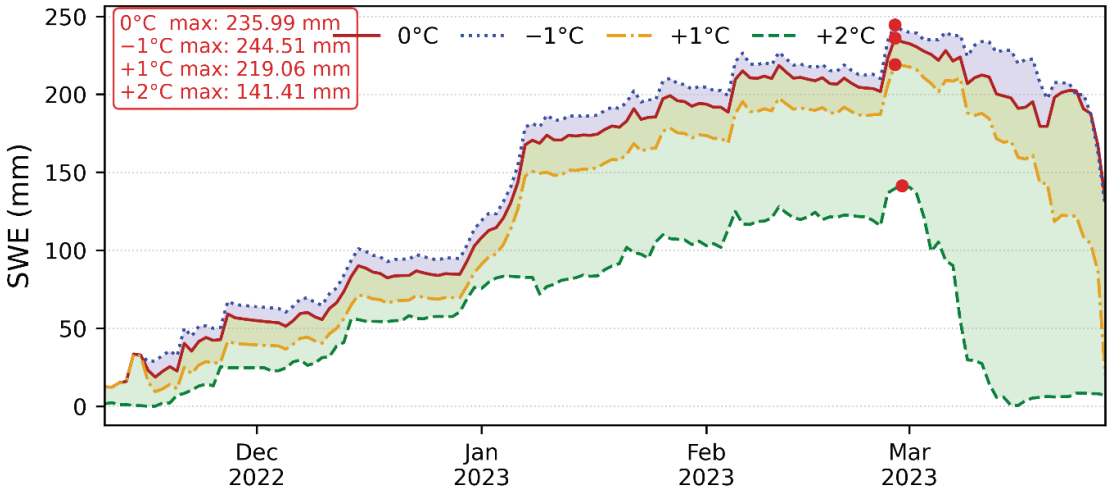

Figure 7. Simulated SWE evolution under additive air temperature offsets (-1 °C, +1 °C, and +2 °C) relative to baseline conditions (0 °C) during the 2022-2023 snow season. Shading highlights the sensitivity of snow accumulation and melt timing to temperature perturbations.

A clear contrast in peak SWE values and melt onset timing is observed across the temperature offset scenarios (Table 4). The baseline (0 °C offset) simulation reaches a peak SWE of approximately 236 mm in early March. The -1 °C cooling scenario yields the highest SWE peak of approximately 244 mm, with melt onset delayed by approximately 5-10 days relative to the baseline. In contrast, the +2 °C warming scenario results in an early and strongly reduced peak of approximately 141 mm, occurring in late February, roughly 15-20 days earlier than the baseline. These results highlight the strong nonlinear sensitivity of seasonal snow storage to modest warming near the freezing threshold. The temporal evolution of SWE across scenarios is illustrated in Fig. 7.

Table 4. Summary of SWE peak values and melt onset timing under temperature perturbation scenarios

Scenario	Peak SWE (mm)	Peak Timing	Melt Onset Shift
−1 °C Cooling	~244 mm	Early March (~Mar 5–7)	+5 to +10 days (later)
Baseline (0 °C)	~236 mm	Early March (~Mar 3–5)	Reference
+1 °C Warming	~219 mm	Late February – Early March	−5 to −10 days (earlier)
+2 °C Warming	~141 mm	Late February (~Feb 18–22)	−15 to −20 days (earlier)

Peak SWE shows a clear contrast across temperature perturbation scenarios (Table 4). Cooling by −1 °C produced only a minor increase relative to baseline conditions, whereas warming caused progressively stronger reductions in snow storage. Peak SWE decreased from approximately 236 mm in the baseline simulation to approximately 141 mm under +2 °C warming, corresponding to an approximate 40% reduction. This asymmetric response reflects the strong nonlinear sensitivity of seasonal snow storage to modest warming near the freezing threshold.

To further investigate the physical mechanism of snowmelt under subfreezing air temperature conditions, surface snow temperature and surface energy balance components were analysed (Fig. 8). This analysis provides mechanistic evidence linking melt onset to positive net surface energy and snow surface temperature approaching the melting point.

Scientific Journal of Astana IT University
ISSN (P): 2707-9031 ISSN (E): 2707-904X
VOLUME 25, MARCH 2026

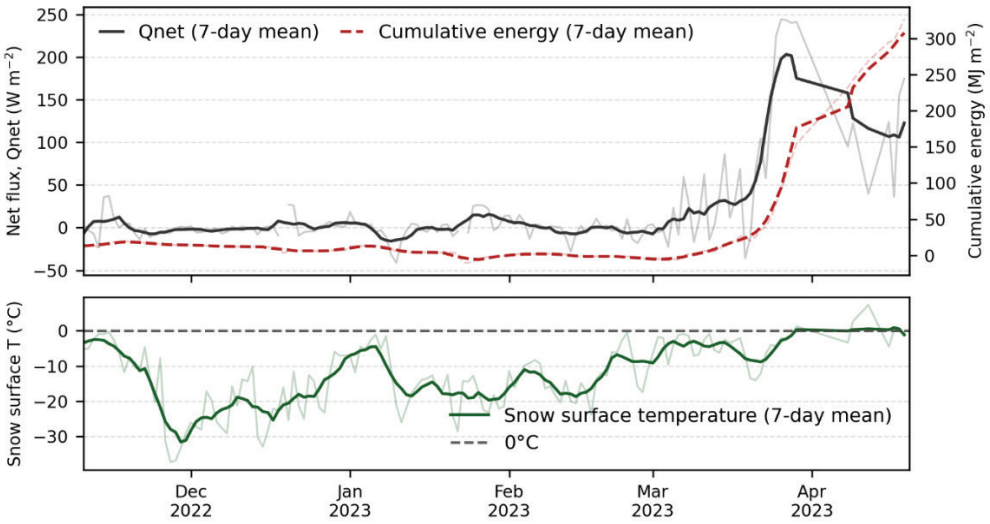

Figure 8. Net surface energy flux (Qnet), cumulative surface energy, and snow surface temperature during the 2022–2023 snow season. Melt periods coincide with rapid energy accumulation and surface temperature approaching 0 °C, indicating energy-balance control.

Results indicate that melt onset is primarily controlled by positive net radiative and turbulent energy inputs. Snow metamorphism affects snow physical properties such as albedo, thermal conductivity, and permeability, but does not directly supply melt energy.

Discussion

The results of this study demonstrate the strong performance and practical value of the SNTHERM model for simulating snowpack evolution in data-scarce continental climates such as East Kazakhstan. SNTHERM's physically based structure enables it to capture key thermodynamic processes, including vertical snow layering, compaction, meltwater percolation, refreezing, and internal energy redistribution, which are often oversimplified in empirical temperature-index models. Its ability to reproduce seasonal snow accumulation, peak SWE, and melt onset with good agreement to observations, despite limited in situ measurements, highlights its applicability for operational snow modelling and climate impact assessments in regions with sparse ground monitoring.

Beyond its ability to reproduce observed seasonal behaviour, SNTHERM demonstrates a physically consistent response to moderate thermal perturbations. The temperature sensitivity experiments revealed nonlinear but physically interpretable shifts in snowpack timing and magnitude in response to modest air temperature changes. Warming scenarios produced substantial reductions in peak SWE and earlier melt onset, while cooling scenarios increased SWE storage and delayed melt timing. Such behaviour is particularly relevant in continental environments, where winter temperatures frequently occur near the freezing threshold and small climatic shifts can substantially modify snow accumulation and melt trajectories.

Part of the simulated temperature sensitivity is linked to precipitation phase partition near the freezing point. In continental climates, precipitation events frequently occur under near-freezing atmospheric conditions, where small temperature deviations can alter the rain–snow ratio. Sensitivity experiments using alternative rain–snow thresholds (−1 °C and +1 °C) demonstrate that precipitation phase partition assumptions influence SWE magnitude, particularly during transitional temperature periods. However, the overall seasonal evolution pattern and temperature sensitivity behaviour remain robust across tested threshold scenarios.

Physically based snow modelling provides mechanistic diagnostics of snowpack processes and can outperform empirical temperature-index approaches when appropriately forced and evaluated. In this study, comparisons between SNTHERM and the degree-day factor (DDF) model highlight structural differences between energy-balance and temperature-index modelling approaches rather than absolute predictive accuracy. This makes SNTHERM particularly suitable for supporting decision-making in water resource management, flood forecasting, and seasonal planning in snowmelt-dominated river basins, while acknowledging that results represent process-level understanding at the study site scale.

Nevertheless, several limitations must be acknowledged. Model performance depends on the accuracy of input meteorological forcing. While ERA5-Land provides physically consistent and spatially complete forcing fields, uncertainties remain in key variables such as near-surface temperature, precipitation phase, and solid precipitation intensity. While sublimation was not explicitly quantified in this study, previous work in similar continental environments suggests that sublimation losses during peak melt periods are typically small relative to melt-driven mass loss. However, sublimation may be locally enhanced under windy and dry conditions and may contribute additional mass loss outside peak melt periods.

In addition, SNTHERM does not explicitly represent lateral snow redistribution processes such as wind-driven transport or subgrid-scale terrain effects, which may influence local SWE variability in complex terrain. The study site represents low-elevation continental snow conditions typical of valley-floor environments in the Irtysh basin. Snow accumulation and retention at this location are influenced by local terrain shielding and reduced wind exposure compared to upland or exposed ridge environments. Wind-driven snow redistribution and subgrid terrain heterogeneity are not explicitly represented in the 1D SNTHERM framework and may contribute to spatial SWE variability at larger scales. Therefore, extrapolation of results to complex terrain or high-elevation zones should be performed cautiously.

The comparison with the degree-day factor (DDF) model should also be interpreted carefully. In this study, DDF parameters were calibrated using SNTHERM-derived melt rather than independent observational melt estimates. Therefore, the DDF model should be interpreted as a simplified statistical emulator of SNTHERM behaviour rather than an independently validated predictive model. The SNTHERM–DDF comparison is therefore intended to illustrate structural differences between physically based energy-balance modelling and temperature-index approaches, rather than to provide an independent accuracy assessment against observations.

Despite these limitations, the demonstrated agreement between SNTHERM simulations and observed SWE dynamics, combined with physically consistent sensitivity responses, indicates that SNTHERM provides a robust framework for diagnosing snowpack responses to climatic variability. These findings are consistent with results reported for other cold continental regions, supporting the broader applicability of physically based snow models in data-limited environments.

Future work should expand sensitivity analyses to include precipitation variability, radiation forcing changes, and wind effects, and should couple SNTHERM with hydrological routing models for basin-scale runoff prediction. Integration of high-resolution remote sensing products and downscaled climate projections may further improve model initialization, evaluation, and long-term scenario analysis, strengthening the role of SNTHERM as a diagnostic and predictive tool for managing snow-dependent water resources under ongoing climate change.

Conclusion

This study has demonstrated that the physically based SNTHERM model, when forced with ERA5-Land reanalysis data, is capable of accurately simulating snowpack evolution in a continental climate regime with limited in situ data. Applied over East Kazakhstan, SNTHERM effectively reproduced key features of seasonal snow dynamics-including the timing and magnitude of accumulation, peak snow water equivalent (SWE), and melt onset—with high statistical agreement to ground-based observations. These results validate the model's suitability for operational snowpack monitoring and hydrological assessment in data-sparse cold regions.

The sensitivity analysis revealed that even modest temperature perturbations (±2-5%) produce substantial, nonlinear changes in snowpack behavior, with earlier or delayed melt onset by up to three weeks and peak SWE deviations exceeding 25%. This high thermal sensitivity, combined with the model's ability to resolve internal snowpack processes, underscores the critical role of physically based models in capturing snow-climate interactions that simpler empirical approaches often overlook.

By applying SNTHERM in a transitional snow climate, this study highlights its added value not only for current snowpack estimation but also for scenario analysis under climate change. The model's responsiveness and physical fidelity make it a valuable diagnostic tool for exploring future snowpack vulnerabilities, informing water resource planning, and supporting early warning systems in snow-dominated basins.

Looking forward, expanding this work to incorporate additional climatic variables, distributed modeling frameworks, and coupling with hydrological routing systems will enhance the applicability of

Scientific Journal of Astana IT University
ISSN (P): 2707-9031 ISSN (E): 2707-904X
VOLUME 25, MARCH 2026

SNTHERM for basin-scale decision support. As climate change continues to reshape snow regimes worldwide, robust, process-based snow models will be essential tools for anticipating and managing future hydrological risks in cold-region catchments.

Acknowledgment

This work has been funded by the Science Committee of the Ministry of Science and Higher Education of the Republic of Kazakhstan (Grant Number BR24992899) within the framework of the project «Development of a system for forecasting catastrophic floods in the East Kazakhstan region using remote sensing data, GIS technologies, and machine learning».

References

[1] Musselman, K. N., Addor, N., Vano, J. A., & Molotch, N. P. (2021). Winter melt trends portend widespread declines in snow water resources. *Nature Climate Change, 11*, 418–424. https://doi.org/10.1038/s41558-021-01014-9

[2] Jin, Z., Qin, X., Li, X., Zhao, Q., Zhang, J., Ma, X., Wang, C., He, R., & Wang, R. (2025). Quantitative analysis of factors driving the variations in snow cover fraction in the Qilian Mountains, China. *Journal of Arid Land, 17*, 888–911. https://doi.org/10.1007/s40333-025-0083-x

[3] Sarker, S. K., Zhu, J., Fryar, A. E., & Jeelani, G. (2023). Hydrological functioning and water availability in a Himalayan karst basin under climate change. Sustainability, 15(11), 8666. https://doi.org/10.3390/su15118666

[4] Sturm, M., Goldstein, M. A., & Parr, C. (2017). Water and life from snow: A trillion dollar science question. *Water Resources Research*, 53(5), 3534- 3544. https://doi.org/10.1002/2017WR020840

[5] Mott, R., Winstral, A., Cluzet, B., Helbig, N., Magnusson, J., Mazzotti, G., Quéno, L., Schirmer, M., Webster, C., & Jonas, T. (2023). Operational snow-hydrological modeling for Switzerland. *Frontiers in Earth Science, 11*, 1228158. https://doi.org/10.3389/feart.2023.1228158

[6] Chen, Y., Li, Z., Fang, G., & Deng, H. (2017). Impact of climate change on water resources in the Tianshan Mountains, Central Asia. *Acta Geographica Sinica, 72*(1), 18–26. https://doi.org/10.11821/dlxb201701002

[7] Kauazov, A. M., Tillakarim, T. A., Salnikov, V. G., & Polyakova, S. E. (2023). Assessment of changes in snow cover area in Kazakhstan from 2000 to 2022. *Sovremennye Problemy Distantsionnogo Zondirovaniya Zemli iz Kosmosa*, 20(1), 298-305. https://doi.org/10.21046/2070-7401-2023-20-1-298-305

[8] Muñoz-Sabater, J., Dutra, E., Agustí-Panareda, A., Albergel, C., Arduini, G., Balsamo, G., et al. (2021). ERA5-Land: A state-of-the-art global reanalysis dataset for land applications. *Earth System Science Data*, 13(9), 4349-4383. https://doi.org/10.5194/essd-13-4349-2021

[9] Wu, X., Su, J., Ren, W., Lü, H., & Yuan, F. (2023). Statistical comparison and hydrological utility evaluation of ERA5-Land and IMERG precipitation products on the Tibetan Plateau. *Journal of Hydrology*, 620, 129384. https://doi.org/10.1016/j.jhydrol.2023.129384

[10] Shrestha, S., Zaramella, M., Callegari, M., Greifeneder, F., & Borga, M. (2023). Scale dependence of errors in snow water equivalent simulations using ERA5 reanalysis over alpine basins. *Climate*, 11(7), 154. https://doi.org/10.3390/cli11070154

[11] Daly, S. F., Giovando, J., Hamill, D., Dahl, T., & Bartles, M. (2023). Snowmelt estimation using an empirical radiation model. *Journal of Hydrology, 619*, 129290. https://doi.org/10.1016/j.jhydrol.2023.129290

[12] Zhou, G., Chen, W., & Chen, K. (2021). A review on snowmelt models: Progress and prospect. *Sustainability, 13*(20), 11485. https://doi.org/10.3390/su132011485

[13] Lafaysse, M., et al. (2017). A multiphysical ensemble system of numerical snow modelling. The Cryosphere, 11, 1173–1198. https://doi.org/10.5194/tc-11-1173-2017

[14] Le Moigne, P., Besson, F., Martin, E., Boé, J., Boone, A., Decharme, B., Etchevers, P., Faroux, S., Habets, F., Lafaysse, M., Leroux, D., & Rousset-Regimbeau, F. (2020). The latest improvements with SURFEX v8.0 of the Safran-Isba-Modcou hydrometeorological model for France. *Geoscientific Model Development, 13*, 3925-3946. https://doi.org/10.5194/gmd-13-3925-2020

[15] Kim, R. S., Kumar, S., Vuyovich, C., Houser, P., Lundquist, J., Mudryk, L., Durand, M., Barros, A., Kim, E. J., Forman, B. A., Gutmann, E. D., Wrzesien, M. L., Garnaud, C., Sandells, M., Marshall, H.-P., Cristea, N., Pflug, J. M., Johnston, J., Cao, Y., Mocko, D., & Wang, S. (2020). Snow Ensemble Uncertainty Project (SEUP):

Quantification of snow water equivalent uncertainty across North America via ensemble land surface modeling. *The Cryosphere Discussions*. https://doi.org/10.5194/tc-2020-248

[16] Hao, X., Huang, G., Zheng, Z., Sun, X., Ji, W., Zhao, H., Wang, J., Li, H., & Wang, X. (2022). Development and validation of a new MODIS snow-cover-extent product over China. *Hydrology and Earth System Sciences, 26*(8), 1937–1952. https://doi.org/10.5194/hess-26-1937-2022

[17] Wrzesien, M. L., Durand, M. T., Pavelsky, T. M., Kapnick, S. B., Zhang, Y., Guo, J., & Shum, C. K. (2019). A new estimate of North American mountain snow accumulation from regional climate model simulations. *Geophysical Research Letters*, 45(3), 1423-1432. https://doi.org/10.1002/2017GL076664

[18] Bonsoms, J., López-Moreno, J. I., Lemus-Canovas, M., & Oliva, M. (2024). Future winter snowfall and extreme snow events in the Pyrenees. *SSRN*. https://doi.org/10.2139/ssrn.4756048

[19] Krinner, G., Derksen, C., Essery, R. L. H., Flanner, M., & others. (2018). ESM-SnowMIP: Assessing snow models and quantifying snow-related climate feedbacks. *Geoscientific Model Development, 11*(12), 5027–5049. https://doi.org/10.5194/gmd-11-5027-2018

[20] Stigter, E. E., Steiner, J. F., Koch, I., Saloranta, T. M., Kirkham, J. D., & Immerzeel, W. W. (2021). Energy and mass balance dynamics of the seasonal snowpack at two high-altitude sites in the Himalaya. *Cold Regions Science and Technology, 183*, 103233. https://doi.org/10.1016/j.coldregions.2021.103233

[21] Jennings, K. S., Winchell, T. S., Livneh, B., & Molotch, N. P. (2018). Spatial variation of the rain-snow temperature threshold across the Northern Hemisphere. *Nature Communications*, 9, 1148. https://doi.org/10.1038/s41467-018-03629-7

[22] Dai, Y., Xin, Q., Wei, N., Zhang, Y., Shangguan, W., Yuan, H., et al. (2019). A global high-resolution data set of soil hydraulic and thermal properties for land surface modeling. *Journal of Advances in Modeling Earth Systems, 11*(9), 2996–3023. https://doi.org/10.1029/2019MS001784

[23] Althoff, D., & Rodrigues, L. N. (2021). Goodness-of-fit criteria for hydrological models: Model calibration and performance assessment. *Journal of Hydrology, 600*, 126674. https://doi.org/10.1016/j.jhydrol.2021.126674

[24] Girons Lopez, M., Vis, M. J. P., Jenicek, M., Griessinger, N., & Seibert, J. (2020). Assessing the degree of detail of temperature-based snow routines for runoff modelling in mountainous areas in central Europe. *Hydrology and Earth System Sciences, 24*, 4441–4461. https://doi.org/10.5194/hess-24-4441-2020

[25] Di Marco, N., Avesani, D., Righetti, M., Zaramella, M., Majone, B., & Borga, M. (2021). Reducing hydrological modelling uncertainty by using MODIS snow cover data and a topography-based distribution function snowmelt model. *Journal of Hydrology, 597*, 126020. https://doi.org/10.1016/j.jhydrol.2021.126020

[26] Wang, Y., Wang, J., Xie, J., & Lu, H. (2022). Improvements in the degree-day model, incorporating forest influence, and taking China's Tianshan Mountains as an example. *Journal of Hydrology: Regional Studies, 44*, 101215. https://doi.org/10.1016/j.ejrh.2022.101215